Hindawi Publishing Corporation
EURASIP Journal on Wireless Communications and Networking
Volume 2007, Article ID 19728, 9 pages
doi:10.1155/2007/19728

Research Article

Characteristics of MIMO-OFDM Channels in Indoor Environments

Hajime Suzuki, Thi Van Anh Tran, and Iain B. Collings

Wireless Technologies Laboratory, CSIRO ICT Centre, P.O. Box 76, Epping NSW 1710, Australia

Received 1 April 2006; Revised 16 October 2006; Accepted 19 October 2006

Recommended by Merouane Debbah

We present the results of multiple-input multiple-output orthogonal frequency-division multiplexing (MIMO-OFDM) channel measurements. The measurements were performed in indoor environments using four transmitters and four receivers with 40 MHz bandwidth at 5.25 GHz. Our measurements reveal two-dimensional small-scale fading, and correlation between MIMO subchannels. In the line-of-sight (LoS) case, the MIMO-OFDM channel capacity is found to be strongly dependent on the local scattering environment; and much less dependent in the non-LoS (NLoS) case. Also, MIMO channel capacity is found to be largely uncorrelated over 20 MHz in NLoS, while a strong correlation is found over 40 MHz in some LoS environments. The validity of the conventional Kronecker correlation channel model is tested, along with a recently proposed joint correlation model. The effects of varying antenna element spacing are also investigated, taking into account such effects as mutual coupling, radiation efficiency, and radiation pattern.

1. INTRODUCTION

Multiple-input multiple-output orthogonal frequency-division multiplexing (MIMO-OFDM) is currently being considered as a strong candidate for the physical layer transmission scheme of next generation wireless communication systems [1]. A commercial product utilizing two transmit antennas and three receive antennas (denoted by 2×3) achieving 6 bps/Hz bandwidth efficiency for wireless local area networks (WLAN) is currently available, while the WLAN standardization group is aiming to achieve 15 bps/Hz bandwidth efficiency using four transmitters (Txs) [2].

In this paper, we focus on measuring and characterizing practical MIMO-OFDM channels in indoor environments. Extensive narrowband indoor MIMO channel measurements have been performed by several groups (e.g., [3, 4]); however MIMO-OFDM system design requires an understanding of MIMO channels as a function of frequency. Channel measurements for a 2×2 MIMO-OFDM system at 3.65 GHz with 20 MHz bandwidth have been performed by Motorola in an indoor laboratory environment, as reported in [5]. They provided plots of MIMO subchannel frequency responses showing the differences in line-of-sight (LoS) and non-LoS (NLoS). A full-rank channel matrix was observed across the entire 20 MHz band, even for the case of the LoS path, which the authors regarded was due to many reflectors inside their laboratory.

In [6], 8×8 MIMO-OFDM channels were measured at 5.2 GHz with 120 MHz of bandwidth, at 20 locations in an open-plan office. While the measured channels were utilized in packet error rate simulation to investigate the performance of different modulation and coding schemes, no analysis on the channels, in terms of fading characteristics or MIMO subchannel correlation properties, was reported.

A wideband 8×8 MIMO channel measurement was also reported in [7] where five NLoS paths were analyzed to develop a wideband MIMO channel model. Although full 8×8 MIMO channels were obtained, the authors utilized only their subsets (2×2 and 3×3) in developing the channel model.

A 2×2 MIMO-OFDM channel measurement conducted by NTT at 5.2 GHz using 10 MHz bandwidth is reported in [8], where the channels were measured every 5 mm along measurement routes in an anechoic chamber and four different indoor environments. The measured channels were analyzed in terms of Demmel condition number [9], with smaller Demmel condition number (more suitable for spatial

multiplexing) being observed when polarization diversity was utilized.

Preliminary 2×2 MIMO-OFDM channel measurement results at 2.4 GHz with 16 MHz bandwidth are reported in [10]. Graphs of frequency responses within short time scale (200 milliseconds) measured in NLoS office environment were presented.

In [11], 2×2 MIMO-OFDM channels were measured at 5.25 GHz with a bandwidth of 25 MHz for 200 locations along traveling paths indoors, with steps larger than a wavelength in order to obtain independent channel realizations. Within a laboratory environment, the LoS and NLoS channels did not show significant differences in terms of the condition number, which is the ratio of the smallest and largest singular values of MIMO channel matrix. The authors postulate that this is consistent with the intuition that there are many reflectors in a laboratory environment which make the channels independently frequency-selective.

In this paper, we consider 4×4 MIMO-OFDM with 40 MHz bandwidth. Interestingly, there is a complete lack of currently available measurement sets for this scenario. This is particularly surprising considering that this is precisely the combination which is suggested for providing the maximum data rate in the new IEEE 802.11n standard [2]. In this paper, we systematically investigate the spatial characteristics of the channels in a number of indoor local areas. We show that the channel can change as a function of antenna location in the order of a fraction of a wavelength in these multipath environments. Our measurements reveal two-dimensional small-scale fading, and correlation between MIMO subchannels. The validity of the conventional Kronecker correlation channel model is tested, along with a recently proposed joint correlation model. We show certain inconsistencies in the case of LoS environments, which point to the need for further model development. The effects of varying antenna element spacing are also investigated, taking into account such effects as mutual coupling, radiation efficiency, and radiation pattern.

The paper is organized as follows. The description of the measurement equipment and the measurement site is given in Section 2. Section 3 provides the definition of a MIMO-OFDM channel and its associated theoretical capacity. The results of the MIMO-OFDM channel measurement and corresponding analysis are given in Section 4, followed by the conclusions in Section 5.

2. MEASUREMENT EQUIPMENT AND SITE

The CSIRO ICT Centre has recently developed a 4×4 MIMO-OFDM hardware demonstrator as shown in Figure 1. It operates at 5.25 GHz and supports an operational bandwidth of up to 40 MHz. The receiving antennas are connected to an antenna array positioner controlled by a PC. For channel measurements, the antenna positioner moves the receiving antenna array within a horizontal two-dimensional area of 4 wavelengths $\times$ 4 wavelengths with 0.05 wavelength increment, resulting in 6400 locations. We found that these parameters provided an adequate spatial sampling, based on our observation that from a statistical point of view, the measured results are relatively insensitive to coverage area and wavelength spatial sampling distance.

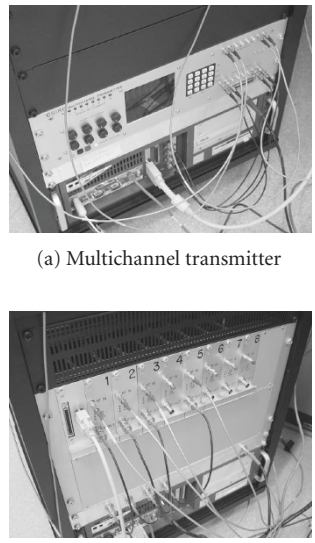

(a) Multichannel transmitter

(b) Multichannel receiver

Figure 1: CSIRO ICT Centre MIMO-OFDM demonstrator.

There is a flexibility to allow a user to perform not only the channel sounding but also testing of different modulation and coding schemes of MIMO-OFDM transmission [12]. Identical off-the-shelf omnidirectional loop antennas (SkyCross SMA-5250-UA) are used as both Tx and Rx antenna array elements for all MIMO-OFDM measurements described in this paper. The antenna elements are arranged to form a uniform square array on the horizontal plane. The spacing of the antenna elements is set to 3 wavelengths at Tx and 2 wavelengths at Rx (except for the measurements described in Section 4.6).

For MIMO-OFDM channel sounding purposes, typically a packet consists of a preamble (for performing packet detection, frame synchronization, and frequency offset correction [13]) and a channel training sequence is sent. The channel training sequence is designed to estimate the frequency response over 117 OFDM subcarriers in a 40 MHz bandwidth with the subcarrier spacing of 312.5 kHz. The choice of OFDM subcarriers is consistent with [2], except that the three middle null carries are also used. To avoid the interference of signals transmitted from different transmitting antennas, the channel training sequence is sent from each transmitting antenna at different times [13]. In order to reduce the effect of noise, the channel training sequence is sent ten times at each location while the estimation of the channel is performed ten times and the averaged results are used for the analysis. A detailed calibration of the system was performed prior to the measurement by directly connecting each of the Txs to each of the Rxs via cables and an attenuator, and measuring the frequency response of each pair of Tx and Rx. The frequency response of the system is subtracted from the measured over-the-air MIMO-OFDM channels. This removes any effects of RF front-end filters in Tx and Rx devices.

(a) Laboratory (b) Atrium (c) Lecture theater

Figure 2: Photographs of measurement sites.

The transmitting power used during the measurement was varied from −10 dBm to 10 dBm per transmitting antenna, depending on the environment and the distance between Tx and Rx. Observed signal-to-noise ratio (SNR) was better than 25 dB in average over frequency. A set of MIMO-OFDM channels in a local area consists of the channel coefficients of 16 MIMO subchannels at 117 OFDM subcarriers at 6400 locations, which amounts to approximately 12 million channels per local area measurement. Currently, this measurement takes approximately 6 hours. The measurement was performed during the night or over the weekend in order to avoid possible temporal variation due to human activities.

The measurements were performed in the CSIRO ICT Centre Laboratory in Marsfield, Sydney. Six propagation links covering both LoS path and NLoS path were established as follows.

(i) LoS 1: both Tx and Rx are located in a laboratory with LoS. Direct distance between Tx and Rx is 5 m.
(ii) LoS 2: both Tx and Rx are located in an atrium with LoS, 7 m.
(iii) LoS 3: both Tx and Rx are located in a lecture theater with LoS, 9 m.
(iv) NLoS 1: Tx is located in an office environment while Rx is located in the laboratory with no LoS, 5 m.
(v) NLoS 2: Tx is located in an office environment while Rx is located in the atrium with no LoS, 10 m.
(vi) NLoS 3: both Tx and Rx are located in office environment with each end in different rooms with no LoS, 9 m.

Photographs of the laboratory, atrium, and lecture theater are shown in Figure 2, by way of example.

3. DEFINITION OF MIMO-OFDM CHANNEL AND CAPACITY

The MIMO-OFDM channel is characterized by its coefficient $g(i, j, k, l)$ defined as the complex ratio of the signal output from the ith receiving antenna over the signal input to the jth transmitting antenna, at the kth OFDM subcarrier, and at the lth receiving antenna array location. The number of transmitting antennas, receiving antennas, OFDM subcarriers, and the receiving antenna array locations is n_t, n_r, n_f, and n_x, respectively. It is convenient to work on the normalized channel coefficient $h(i, j, k, l)$ so that the Shannon capacity of the MIMO channel can be derived as a function of SNR per receiving antenna, averaged over all MIMO subchannels, OFDM subcarriers, and receiving antenna array locations. The convention is to perform normalization at each receiving antenna array location [14], which assumes that the transmitting power can be adjusted without limitations to provide fixed average SNR per Rx. For a practical situation where the transmitting power is limited [3], it is more convenient to define the average SNR per Rx over a local area. In this case, the normalization is performed over a local area as follows:

$$h(i, j, k, l) = \frac{g(i, j, k, l)}{\sqrt{(1/n_t n_r n_f n_x) \sum_{i=1}^{n_r} \sum_{j=1}^{n_t} \sum_{k=1}^{n_f} \sum_{l=1}^{n_x} |g(i, j, k, l)|^2}}. \quad (1)$$

For the current measurement, $n_t = 4$, $n_r = 4$, $n_f = 117$, and $n_x = 6400$. The normalized channel matrix at the kth OFDM subcarrier at the lth receiving antenna array location is given by the channel coefficient matrix $\mathbf{H}(k, l)$ whose ith row and jth column element is $h(i, j, k, l)$. When the MIMO channel is completely known by Rx but is unknown to Tx, the Shannon capacity of the MIMO channel at the kth OFDM subcarrier at the lth receiving antenna array location is given by [15]

$$C(k, l) = \sum_{m=1}^{n_t} \log_2 \left(1 + \frac{\rho}{n_t} \lambda_m(k, l)\right), \quad (2)$$

where ρ is the average SNR per Rx over MIMO subchannels, OFDM subcarriers, and a local area, $\lambda_m(k, l)$ is the mth eigenvalue of $\mathbf{H}(k, l)^H \mathbf{H}(k, l)$, and superscript H denotes complex conjugate transpose. In the following, the MIMO channel capacity is calculated at each OFDM subcarrier using the above equation, while the MIMO-OFDM channel capacity is calculated as an average of MIMO channel capacity over all OFDM subcarriers.

4. MEASUREMENT RESULTS AND ANALYSIS

4.1. Measured MIMO-OFDM channels

Figure 3 shows an example of measured MIMO-OFDM channels. Sets of MIMO-OFDM channels obtained at eight

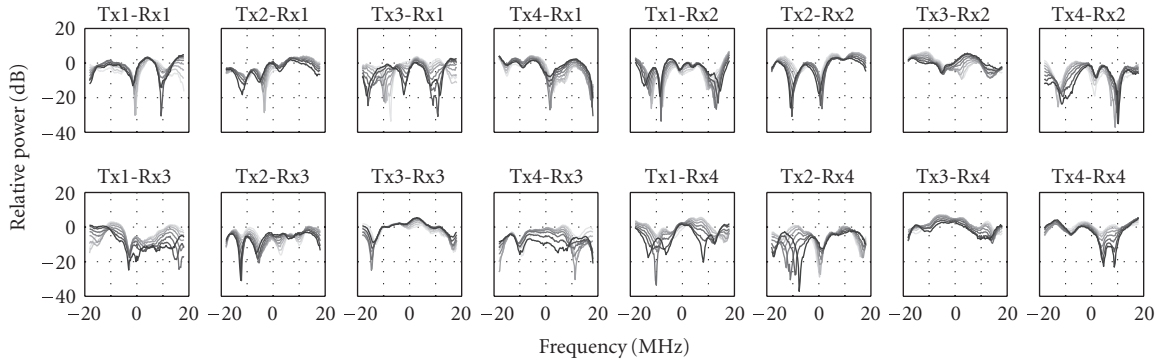

Figure 3: An example of measured MIMO-OFDM frequency response, NLoS 3 (office rooms) path.

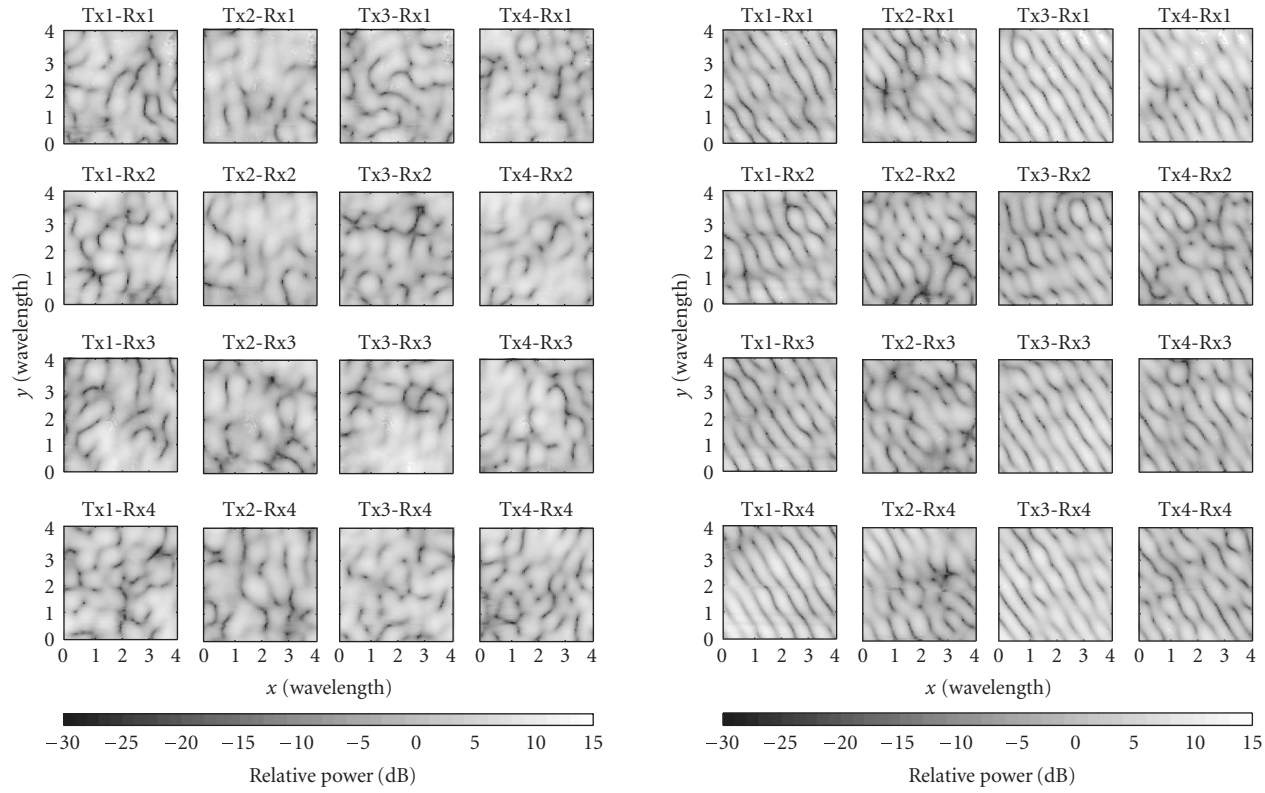

(a) NLoS 3 (office rooms) path

(b) LoS 3 (lecture theater) path

Figure 4: Examples of measured MIMO subchannel fading maps.

consecutive Rx antenna array locations with 0.05-wavelength spacing are plotted (from light gray curves to solid black curves) showing typical variation in space and in frequency. As expected from a multipath environment, severe frequency-selective fading is observed in most MIMO subchannels.

Figure 4 shows examples of the small-scale spatial fading pattern measured with NLoS 3 link and LoS 3 link, respectively, at one of the OFDM subcarriers. (Interested readers are referred to [16] or [17] for the small-scale spatial fading plots in other environments.) Deep fading in the order of 30 dB is commonly observed in both cases, which is a characteristic of the narrowband small-scale spatial fading. An apparent correlation of the different MIMO subchannels is observed in the case of LoS path, for example Tx3-Rx3 and Tx3-Rx4. Such a correlation of MIMO subchannels is known to reduce the MIMO channel capacity [18]. A similar fading pattern was observed for different OFDM subcarriers.

4.2. MIMO subchannel correlations

Correlation analysis is a useful tool in assessing MIMO channels [19]. The complex correlation coefficient ρ of two

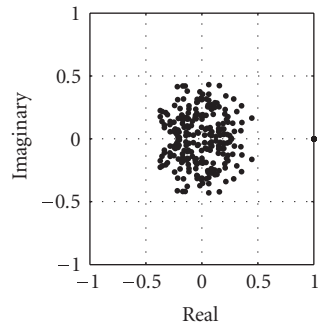

(a) NLoS 2 (atrium)

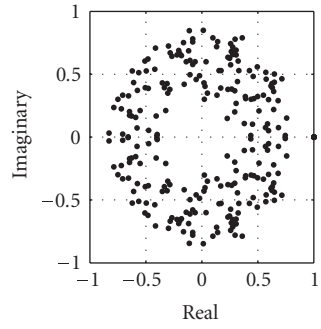

(b) LoS 2 (atrium)

Figure 5: Complex correlation coefficient of 4×4 MIMO channels for one of the OFDM subcarriers.

complex random variables v and u is defined as

$$\rho = \frac{E[uv^*] - E[u]E[v^*]}{\sqrt{\left(E[|u|^2] - |E[u]|^2\right)\left(E[|v|^2] - |E[v]|^2\right)}}, \quad (3)$$

where $*$ denotes the complex conjugate operation. For each of 117 OFDM subcarriers, the complex correlation coefficients of each pair of the 16 MIMO subchannels (e.g., between Tx1-Rx1 channel and Tx1-Rx2 channel) are derived and analyzed in this section.

A plot in Figure 5 shows 256 complex points each of which represents a correlation coefficient of each pair of the 16 MIMO subchannels of a single OFDM subcarrier. Results from NLoS 2 and LoS 2 paths are shown in Figure 5. The spread of points indicates that some pairs of MIMO subchannels are more correlated than others. It is apparent that the magnitude of correlation is larger in the case of the LoS 2 path than the NLoS 2 path, both measured in the atrium. The ring-like plot in Figure 5(b) indicates high fading correlation between channels. This can occur if the dominant propagation paths are not resolved at the chosen antenna spacing. Similar results are observed for other OFDM subcarriers.

Table 1 shows the maximum and the average values of the correlation coefficient amplitude in different environments. The analysis is performed by first removing the autocorrelation of value 1, finding the maximum and the average values for each OFDM subcarrier, then the results are further averaged over all OFDM subcarriers. It is well known that

Table 1: Amplitude of correlation coefficient.

Values	LoS 1	LoS 2	LoS 3	NLoS 1	NLoS 2	NLoS 3
Maximum	0.53	0.87	0.79	0.54	0.52	0.47
Average	0.22	0.62	0.36	0.22	0.23	0.20

the correlation of MIMO subchannels in an indoor NLoS environment is relatively small provided that the antenna elements are sufficiently separated. However, the values are significantly different for the three LoS links. This difference can be attributed to the fact that more objects such as metal cabinets and measurement equipments can be found inside the laboratory (LoS 1) that may cause more scattered waves, whereas very few of such objects are found in the atrium (LoS 2). These differences are found to have a large impact on the performance of MIMO-OFDM systems [17].

The finding of uncorrelated MIMO channels in a laboratory LoS environment is consistent with the findings reported in [5, 11], while reports on measured correlated LoS MIMO channels in an indoor environment, as given in this paper, are scarce in the literature.

4.3. Rician factor

The spatial fading of a narrowband channel in indoor environments is often assumed to be Rayleigh distributed even in LoS link due to many scattering objects surrounding both Tx and Rx. The degree of multipath scattering can be verified by the Rician factor [20] with small Rician factor indicating more scattering. The Rician factor was estimated by the moment-method [21] from the measured MIMO-OFDM channels for each OFDM subcarrier and for each MIMO subchannel. Figure 6 shows the estimated Rician factor in the three LoS environments. (Note that the Rician factor in NLoS environment was observed to be small, mostly smaller than 0 dB.) Large Rician factor values are observed in some of the MIMO subchannels in the atrium while relatively smaller values are seen in the laboratory, which is consistent with the finding in correlation properties discussed above. The figure also indicates some dependency of Rician factor on different MIMO subchannels (different MIMO subchannels experiencing different Rician factors). This indicates that the assumption of identically distributed channels may not often be valid in indoor LoS environment.

4.4. MIMO capacity

Figure 7 shows an example of the small-scale variation of the theoretical MIMO-OFDM channel capacity (SNR = 15 dB) for the LoS 2 link and NLoS 2 link. The MIMO-OFDM channel capacity is an average of MIMO channel capacity over all OFDM subcarriers. It is notable that the channel capacity can vary significantly with a small shift of the receiving antenna array location on the order of a 0.5-wavelength. This indicates that an additional measure to provide further spatial diversity (e.g., receiving antenna selection) may be an effective method.

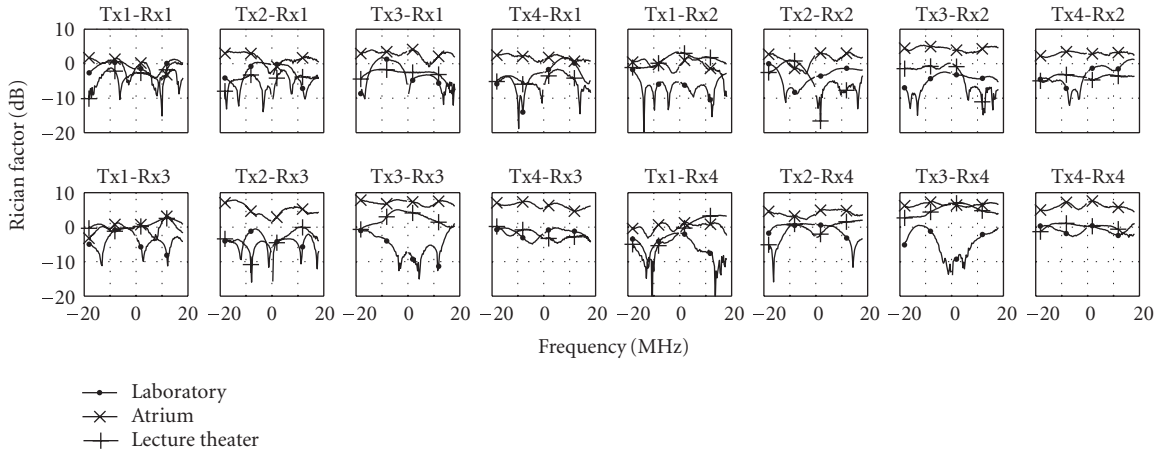

Figure 6: Measured Rician factor for LoS paths in the laboratory, atrium, and lecture theater.

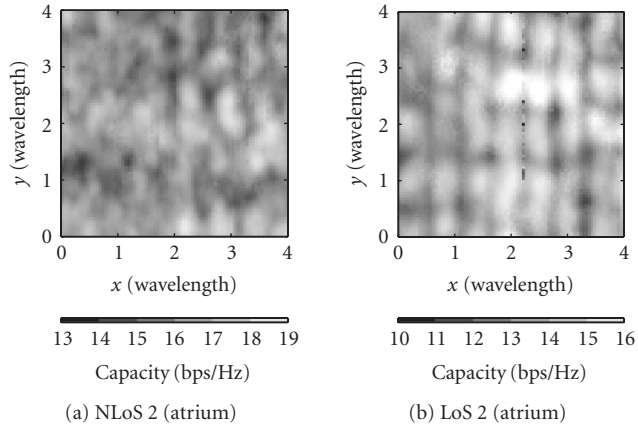

Figure 7: Theoretical 4 × 4 MIMO-OFDM channel capacity (SNR = 15 dB).

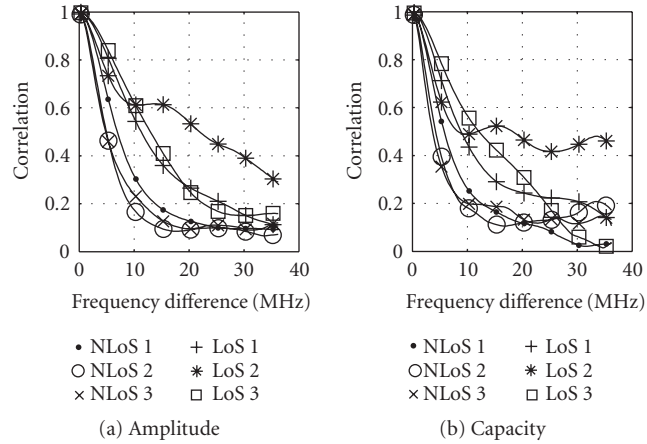

Figure 8: Correlation in frequency.

4.5. Frequency correlation

With the MIMO-OFDM system in a frequency-selective fading environment, additional diversity may be obtained by spreading coded signal in frequency. Figure 8 shows an average correlation of MIMO subchannel amplitude and MIMO channel capacity as a function of OFDM subcarrier frequency differences. The average is performed over different frequency pairs and over different MIMO subchannels in the case of channel amplitude, while it is performed over different frequency pairs in the case of MIMO channel capacity. It is observed that the MIMO channel capacity is largely uncorrelated with a frequency difference of 20 MHz in the case of NLoS paths. However the correlation of the LoS path in the atrium is found to be large over a 40 MHz difference.

4.6. Effects of antenna spacing

The effects of antenna spacing on the performance of MIMO capacity have been investigated by several researchers (e.g., [22–24]). However the complex interaction of mutual coupling between the antenna elements and changes in radiation pattern make an analytical approach difficult. Here we directly measure MIMO-OFDM channels while varying antenna element spacing of the uniform square array from 0.5 wavelengths to 2 wavelengths with 0.5-wavelength steps of (1) both Tx and Rx antenna arrays (referred as Both), and (2) only Rx antenna array (referred as Rx Only). For the second case, the antenna element spacing of the Tx antenna array is fixed at 3 wavelengths. The measurement was performed in LoS 1 and NLoS 1 paths as described in Section 2. For each local area measured, the normalization is performed over all antenna spacings. This method is employed so that in comparing different antenna spacings, the effects of radiation efficiency, mutual coupling, and antenna pattern are all included in the final MIMO-OFDM channel capacity results.

Figure 9 shows cumulative distribution functions (CDFs) of measured MIMO-OFDM channel capacity for different antenna spacings. When the antenna element spacings of both the Tx and Rx antenna arrays are reduced to 1

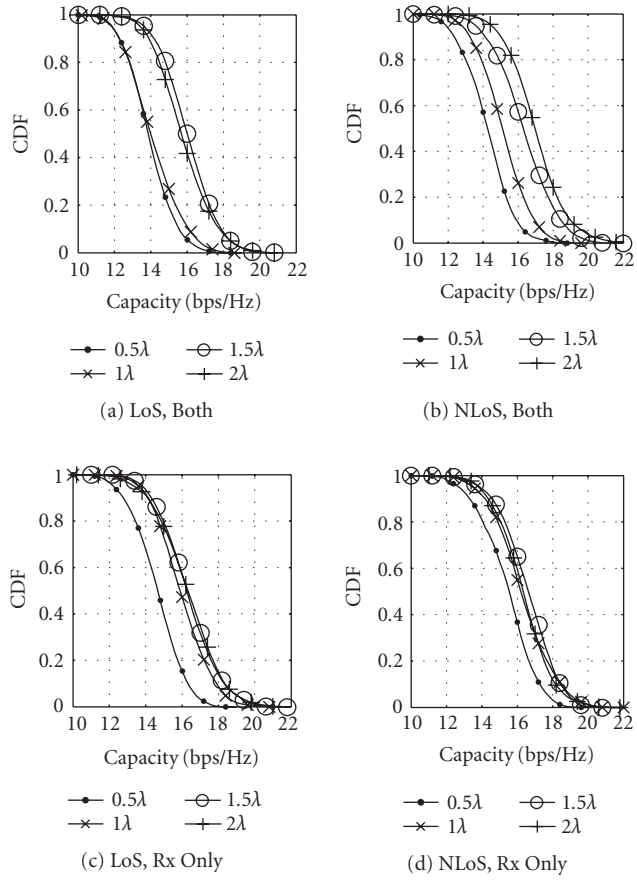

Figure 9: Theoretical 4 × 4 MIMO-OFDM channel capacity (SNR = 15 dB) for different antenna spacing.

wavelength or less, significant degradation of MIMO-OFDM capacity is observed. This contradicts the popular assumption that 0.5 wavelength is sufficient for omnidirectional antennas to obtain close to optimum MIMO channel capacity in indoor environments. In the case where one end has large antenna element separation, 1 wavelength of antenna element spacing for the other end seems to achieve good MIMO channels. Note that the MIMO-OFDM channel capacity is observed to be larger for 1.5-wavelength spacing than for 2-wavelength spacing in the case of LoS Both and NLoS Rx Only. Table 2 shows the average correlation coefficient amplitude (as described in Section 4.2) and average channel gain (over all MIMO subchannels, OFDM subcarriers, and Rx antenna array locations, normalized to the value at 2 wavelength) for different antenna spacings. For those two cases, it can be seen from the table that the average correlation amplitude at 1.5-wavelength spacing is not smaller than that at 2-wavelength spacing, while the average channel gain at 1.5-wavelength spacing is larger than that at 2-wavelength spacing. This indicates that more power was received with 1.5-wavelength spacing, contributing to the gain in the MIMO-OFDM channel capacity. To identify the exact cause of this phenomenon requires a further investigation. However, in general, it can be seen that both the average correlation amplitude and channel gain are less affected in the case of NLoS with larger antenna separation at one end, while a significant variation is observed in the LoS path when the antenna spacings of both Tx and Rx were changed.

4.7. Comparison with stochastic channel models

Stochastic channel models based on correlation properties of MIMO subchannels have been used to simulate realistic correlated MIMO channels. Recently, the suitability of the popular Kronecker model [14, 25, 26] has been questioned for indoor environments [27] when significant correlation is present or the number of Tx/Rx pairs exceed 3 × 3. A new stochastic model based on joint correlation of both link ends (herein called joint correlation model) has been proposed in [28] in order to remedy these deficiencies. However, both models assume that the MIMO subchannels are complex-normal distributed with zero mean, that is, Rayleigh fading. Our analysis on the Rician factor in Section 4.3 shows that the channels in some indoor LoS environments deviate from a Rayleigh distribution. Hence the suitability of the Kronecker model and the novel joint correlation model for LoS and NLoS paths is examined based on the measured channels in this section. MIMO channel realization at 117 OFDM subcarriers and 6400 locations is used to generate the cumulative distribution of MIMO channel capacity in the following analysis.

Figure 10 shows the CDF of measured MIMO channel capacity together with the prediction by the Kronecker and joint correlation models. As previously reported [7], the Kronecker model predicts the MIMO channel capacity relatively well in the case of NLoS paths. However, differences between the Kronecker model and the measured results become apparent for LoS path cases where significant correlation was found (LoS 2 and 3 paths). This confirms the findings reported in [28] that the Kronecker model tends to underestimate the MIMO capacity in LoS path or the number of antennas used in each end becomes larger than 3. While the prediction results from the joint correlation model are always closer to the measured results than those from the Kronecker model, underestimation of the MIMO capacity is still observed. This is attributed to the fact that some of the current measured channels are Rician-distributed. While reports on modeling correlated Rician MIMO channels are appearing in the literature (e.g., [29–31]), those models assume the knowledge of the dominant component, which is difficult to obtain from the current measurement results. Further investigation of a suitable channel model for correlated Rician channel and the method to obtain its parameters from the measurement are called for.

5. CONCLUSIONS

In this paper, the results of MIMO-OFDM channel measurements performed in indoor environments are reported and analyzed. The MIMO-OFDM channel capacity in a local area was found to be strongly dependent on the local scattering environment in the case of an LoS situation, while it is less affected in the case of NLoS situation. The exact structural

Table 2: MIMO channel parameters for different antenna spacings.

Spacing (wavelength)	Average correlation				Average channel gain			
	0.5	1.0	1.5	2.0	0.5	1.0	1.5	2.0
NLos, Rx Only	0.22	0.20	0.19	0.18	1.00	1.04	1.07	1.00
LoS, Rx Only	0.30	0.30	0.30	0.32	0.88	0.96	1.02	1.00
NLoS, Both	0.28	0.25	0.23	0.19	0.79	0.97	1.06	1.00
LoS, Both	0.41	0.31	0.40	0.28	1.01	0.84	1.16	1.00

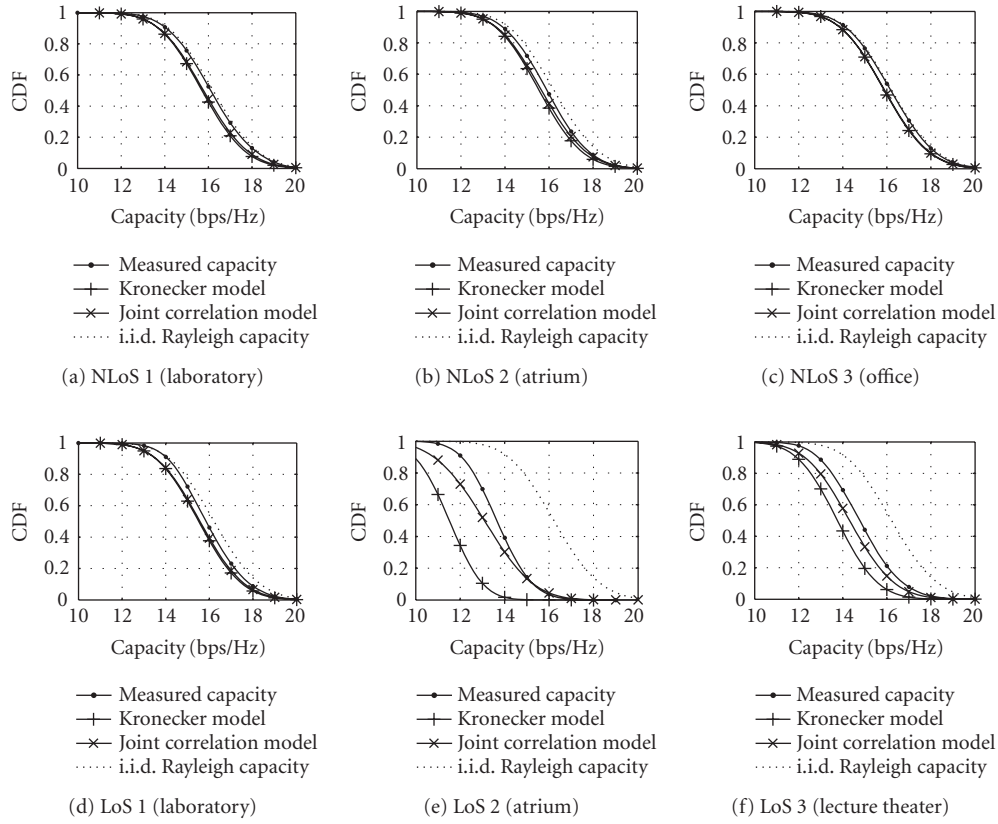

Figure 10: Comparison of measured, Kronecker model, joint correlation model, and i.i.d. Rayleigh capacity CDF.

arrangements that would cause correlation of the MIMO subchannel in indoor LoS environments are still largely unknown. Further measurements with various geometries are required to develop a general model to predict the MIMO-OFDM channel capacity in indoor environments.

REFERENCES

[1] G. L. Stüber, J. R. Barry, S. W. Mclaughlin, Y. E. Li, M. A. Ingram, and T. G. Pratt, "Broadband MIMO-OFDM wireless communications," *Proceedings of the IEEE*, vol. 92, no. 2, pp. 271–293, 2004.

[2] S. Coffey, A. Kasher, and A. Stephens, "Joint Proposal: high throughput extension to the 802.11 Standard: PHY," IEEE 802.11-05/1102r4, January 2006.

[3] P. Kyritsi, D. C. Cox, R. A. Valenzuela, and P. W. Wolniansky, "Effect of antenna polarization on the capacity of a multiple element system in an indoor environment," *IEEE Journal on Selected Areas in Communications*, vol. 20, no. 6, pp. 1227–1239, 2002.

[4] J. W. Wallace, M. A. Jensen, A. L. Swindlehurst, and B. D. Jeffs, "Experimental characterization of the MIMO wireless channel: data acquisition and analysis," *IEEE Transactions on Wireless Communications*, vol. 2, no. 2, pp. 335–343, 2003.

[5] M. D. Batariere, J. F. Kepler, T. P. Krauss, S. Mukthavaram, J. W. Porter, and F. W. Vook, "An experimental OFDM system for broadband mobile communications," in *Proceedings of 54th IEEE Vehicular Technology Conference (VTC '01)*, vol. 4, pp. 1947–1951, Atlantic City, NJ, USA, October 2001.

[6] R. Piechocki, P. Fletcher, A. Nix, N. Canagarajah, and J. McGeehan, "A measurement based feasibility study of space-frequency MIMO detection and decoding techniques for next generation wireless LANs," *IEEE Transactions on Consumer Electronics*, vol. 48, no. 3, pp. 732–737, 2002.

[7] K. Yu, M. Bengtsson, B. Ottersten, D. McNamara, P. Karlsson, and M. Beach, "Modeling of wide-band MIMO radio channels based on NLoS indoor measurements," *IEEE Transactions on Vehicular Technology*, vol. 53, no. 3, pp. 655–665, 2004.

[8] N. Kita, W. Yamada, A. Sato, D. Mori, and S. Uwano, "Measurement of Demmel condition number for 2×2 MIMO-OFDM broadband channels," in *Proceedings of 59th IEEE Vehicular Technology Conference (VTC '04)*, vol. 1, pp. 294–298, Milan, Italy, May 2004.

[9] R. W. Heath Jr. and A. J. Paulraj, "Switching between diversity and multiplexing in MIMO systems," *IEEE Transactions on Communications*, vol. 53, no. 6, pp. 962–968, 2005.

[10] A. Gupta, A. Forenza, and R. W. Heath Jr., "Rapid MIMO-OFDM software defined radio system prototyping," in *Proceedings of IEEE Workshop on Signal Processing Systems Design and Implementation*, pp. 182–187, Austin, Tex, USA, October 2004.

[11] R. M. Rao, S. Lang, and B. Daneshrad, "Indoor field measurements with a configurable multi-antenna testbed," in *Proceedings of IEEE Global Telecommunications Conference (GLOBECOM '04)*, vol. 6, pp. 3952–3956, Dallas, Tex, USA, November-December 2004.

[12] H. Suzuki, R. Kendall, M. Hedley, G. Daniels, and D. Ryan, "Demonstration of 4×4 MIMO data transmission on CSIRO ICT Centre MIMO testbed," in *Booklet of Abstracts for the 6th Australian Communications Theory Workshop*, p. 35, Brisbane, Australia, February 2005.

[13] A. Van Zelst and T. C. Schenk, "Implementation of a MIMO OFDM-based wireless LAN system," *IEEE Transactions on Signal Processing*, vol. 52, no. 2, pp. 483–494, 2004.

[14] K. Yu, M. Bengtsson, B. Ottersten, D. McNamara, P. Karlsson, and M. Beach, "Second order statistics of NLOS indoor MIMO channels based on 5.2 GHz measurements," in *Proceedings of IEEE Global Telecommunicatins Conference (GLOBECOM '01)*, vol. 1, pp. 156–160, San Antonio, Tex, USA, November 2001.

[15] J. H. Winters, "On the capacity of radio communication systems with diversity in a Rayleigh fading environment," *IEEE Journal on Selected Areas in Communications*, vol. 5, no. 5, pp. 871–878, 1987.

[16] H. Suzuki, "Characteristics of 4×4 MIMO-OFDM channels in indoor environments," in *Proceedings of the ClimDiff '05, Diff-13*, Cleveland, Ohio, USA, September 2005.

[17] H. Suzuki, M. Hedley, G. Daniels, and J. Yuan, "Performance of MIMO-OFDM-BICM on measured indoor channels," in *Proceedings of 63rd IEEE Vehicular Technology Conference (VTC '06)*, vol. 5, pp. 2073–2077, Melbourne, Australia, May 2006.

[18] D.-S. Shiu, G. J. Foschini, M. J. Gans, and J. M. Kahn, "Fading correlation and its effect on the capacity of multielement antenna systems," *IEEE Transactions on Communications*, vol. 48, no. 3, pp. 502–513, 2000.

[19] P. Kyritsi, D. C. Cox, R. A. Valenzuela, and P. W. Wolniansky, "Correlation analysis based on MIMO channel measurements in an indoor environment," *IEEE Journal on Selected Areas in Communications*, vol. 21, no. 5, pp. 713–720, 2003.

[20] T. S. Rappaport, *Wireless Communications, Principles & Practice*, Prentice Hall PTR, Upper Saddle River, NJ, USA, 1996.

[21] L. J. Greenstein, D. G. Michelson, and V. Erceg, "Moment-method estimation of the Ricean K-factor," *IEEE Communications Letters*, vol. 3, no. 6, pp. 175–176, 1999.

[22] R. Janaswamy, "Effect of element mutual coupling on the capacity of fixed length linear arrays," *IEEE Antennas and Wireless Propagation Letters*, vol. 1, no. 1, pp. 157–160, 2002.

[23] P. N. Fletcher, M. Dean, and A. R. Nix, "Mutual coupling in multi-element array antennas and its influence on MIMO channel capacity," *Electronics Letters*, vol. 39, no. 4, pp. 342–344, 2003.

[24] J. W. Wallace and M. A. Jensen, "Mutual coupling in MIMO wireless systems: a rigorous network theory analysis," *IEEE Transactions on Wireless Communications*, vol. 3, no. 4, pp. 1317–1325, 2004.

[25] K. I. Pedersen, J. B. Andersen, J. P. Kermoal, and P. Mogensen, "Stochastic multiple-input-multiple-output radio channel model for evaluation of space-time coding algorithms," in *Proceedings of 52nd IEEE Vehicular Technology Conference (VTC '00)*, vol. 2, pp. 893–897, Boston, Mass, USA, September 2000.

[26] J. P. Kermoal, L. Schumacher, K. I. Pedersen, P. E. Mogensen, and F. Frederiksen, "A stochastic MIMO radio channel model with experimental validation," *IEEE Journal on Selected Areas in Communications*, vol. 20, no. 6, pp. 1211–1226, 2002.

[27] H. Özcelik, M. Herdin, W. Weichselberger, J. Wallace, and E. Bonek, "Deficiencies of 'Kronecker' MIMO radio channel model," *Electronics Letters*, vol. 39, no. 16, pp. 1209–1210, 2003.

[28] W. Weichselberger, M. Herdin, H. Özcelik, and E. Bonek, "A stochastic MIMO channel model with joint correlation of both link ends," *IEEE Transactions on Wireless Communications*, vol. 5, no. 1, pp. 90–100, 2006.

[29] S. K. Jayaweera and H. V. Poor, "On the capacity of multiple-antenna systems in Rician fading," *IEEE Transactions on Wireless Communications*, vol. 4, no. 3, pp. 1102–1111, 2005.

[30] M. R. McKay and I. B. Collings, "General capacity bounds for spatially correlated Rician MIMO channels," *IEEE Transactions on Information Theory*, vol. 51, no. 9, pp. 3121–3145, 2005.

[31] M. Kang and M.-S. Alouini, "Capacity of MIMO Rician channels," *IEEE Transactions on Wireless Communications*, vol. 5, no. 1, pp. 112–122, 2006.